Modelling of Evapotranspiration in an Urban Watershed Using Advanced GIS Delineation

Tatsuya KOGA[1], Akira KAWAMURA[2], Hideo AMAGUCHI[2] and Hiroto TANOUCHI[2]

[1] CTI Engineering Co; Ltd, 3-21-1, Nihonbashihamacho, Chuo-ku, Tokyo 103-8430, Japan

[2] Graduate school of Urban Environmental Engineering, Tokyo Metropolitan University, 1-1, Minamiosawa, Hachioji city, Tokyo 192-0397, Japan

Corresponding author's e-mail: t-koga@ctie.co.jp, phone:+81-3-3668-0352

1 INTRODUCTION

Evapotranspiration is affected by soil moisture in areas where infiltration occurs. However, soil moisture is not considered for calculating the evapotranspiration in the common method when estimating the possibility of evaporation capacity used only weather conditions and multiplied by the empirical coefficient with Hamon equation (1961) or Thornthwaite equation (1948). Therefore, using the above formulas, it is not possible to consider how permeable and impermeable land use types or differing soil moisture contents in the various permeable areas may impact on evapotranspiration. Moreover, these equations do not take heat balance aspects into account. In order to accurately calculate the surface temperature, evapotranspiration must be estimated based on latent heat and sensible heat using a heat balance equation (Koga *et al.*, 2013).

The authors (Amaguchi *et al.*, 2007) have built a geographic information system (GIS), based on standard GIS feature data that allows us to classify urban land uses and estimate their infiltration characteristics using new information about the permeable areas. The authors have also described GIS data that faithfully reflects the shapes of features so they can be applied to distributed flood runoff models. The authors also described how to create this type of data, called "advanced GIS delineation", and used the process to produce a detailed discrimination of land use in the Upstream Kanda Watershed (Amaguchi *et al.*, 2009).

To this point, the authors have classified parcels of land into permeable and impermeable areas at the ground surface using advanced GIS delineation and proposed the TET (Tokyo EvapoTranspiration) model, which considers the heat balance due to differences in the earth surface soil moisture and infiltration characteristics (Koga *et al.*, 2014).

In this paper, we apply the TET model to the Upstream Kanda Watershed of Tokyo Japan, which is highly urbanized, using observed temperature data from METROS (Metropolitan Environmental Temperature and Rainfall Observation System). We calculated daily evapotranspiration and the average temperature of each land-surface feature. Using these results, we evaluated how temperatures in the river watershed and land uses affect the spatial distribution of evapotranspiration and surface temperatures in the features.

2 MATERIALS AND METHODS

2.1 Overview – Evapotranspiration model (TET MODEL)

Equations (1) - (3) are the basic equations for the heat balance at the ground surface. They are used to estimate latent and sensible heat, and evapotranspiration is calculated from the estimated latent heat. Equation (4) is a formula for calculating evapotranspiration efficiency β.

$$R_n = H + \ell E + G \tag{1}$$

$$H = c_P \rho \, C_H U(T_s - T) \tag{2}$$

$$\ell E = \ell \, \rho \;\; \beta \, C_H U(q_{SAT} - q) \tag{3}$$

$$\beta = 1 - \frac{2}{1 + \exp(-k \times \lambda_x)} \tag{4}$$

where R_n is net radiation (W/m^2), H is net radiation underground heat transfer (W/m^2), ℓE is sensible heat transfer (W/m^2), G is latent heat transfer (W/m^2), T_S is the earth's surface temperature (K), c_P is the constant pressure specific heat of air (1005 J/kg/K), ρ is the density of air (kg/m^3), C_H is the bulk coefficient of sensible heat transport (dimensionless), U is the wind speed at the observation point (m/s), T is air temperature (K), ℓ is the latent heat of vaporization of water (2.50 × 10^6 J/kg), β is evapotranspiration efficiency (dimensionless), q_{SAT} is the saturation specific humidity for T_S (dimensionless), q is the atmosphere's specific humidity (dimensionless), k is the evapotranspiration coefficient to be set for each land use type (dimensionless) and λ_x is the soil moisture coefficient (dimensionless).

In permeable areas, the TET model can estimate evapotranspiration and consider differences in soil moisture in each land use type. The model use sensible heat and latent heat calculated from the evaporation efficiency β which represents the ease of evaporation in the bulk formula. β is calculated from the soil moisture and evapotranspiration coefficients of each land use type. Permeable areas are modeled using a Soil Moisture Parameter Tank (SMPT) model that is built to simulate the process of infiltration in the surface soil, and impermeable areas are modeled so that depression storage in those areas is accounted for (Koga *et al.*, 2013).

2.2 Overview of Kanda Upstream Watershed

In this paper, we investigate a watershed area of about 11.5 km^2 which encompasses a flow path about 9 km long, extending from the Inokashira Pond to the confluence of the Zenpukuji River with the Kanda River as shown in Fig. 1. Fig. 2 shows the advanced GIS delineation of the Upstream Kanda Watershed with its features classified into 20 land use types.

The number of elements and the proportions of surface features of various types provided by advanced GIS delineation (Amaguchi *et al*., 2011) data are shown in Table 1. The table shows that there are 104,342 elements in the surface feature data. The largest land use types are *Between roads* and *Building*, at about 30% each, followed by *Road* at about 16%, and

Forest at about 9% of the area. These four types account for about 84% of the total land use.

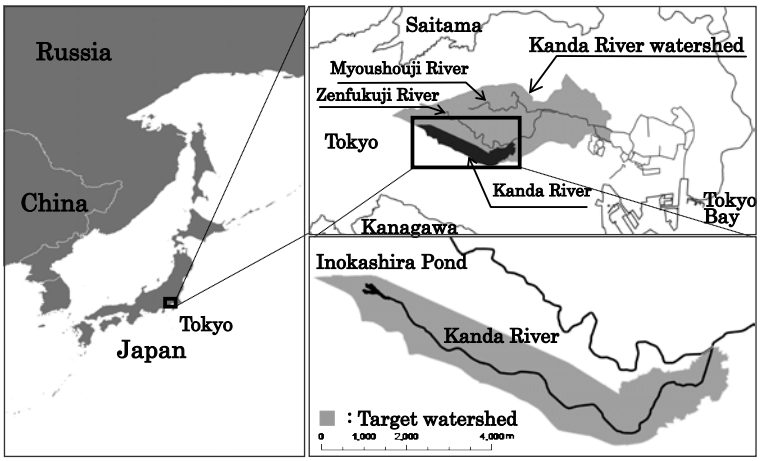

Figure 1. Upstream Kanda Watershed location map

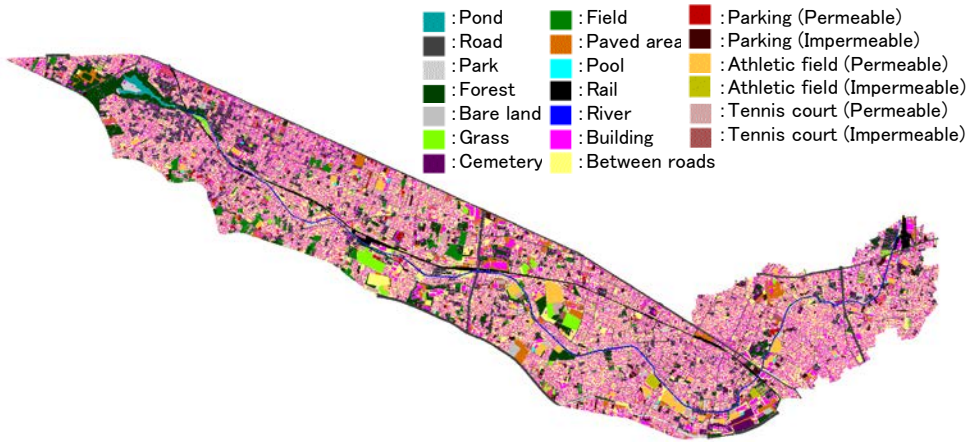

Figure 2. Advanced GIS delineation of the Upstream Kanda Watershed

Table 1. Numbers of advanced GIS delineation elements and area percentages by land use type

No.	Advanced GIS delineation land use type	Number of Features	Area (m^2)	Area ratio (%)
1	Building	34,054	3,382,235	29.39
2	Parking (Permeable)	177	60,351	0.52
3	Parking (Impermeable)	635	207,213	1.80
4	Athletic field (Permeable)	568	225,656	1.96
5	Athletic field (Impermeable)	48	23,288	0.20
6	Forest	3,185	1,041,020	9.05
7	Grass	409	171,526	1.49
8	Field	483	188,587	1.64
9	Park	310	104,735	0.91
10	Cemetery	171	70,392	0.61
11	Paved area	1,157	379,521	3.30
12	Rail	570	149,388	1.30
13	Between roads	16,765	3,432,446	29.83
14	Tennis court (Permeable)	108	54,613	0.47
15	Tennis court (Impermeable)	62	30,383	0.26
16	Bare land	117	52,714	0.46
17	Pool	27	11,750	0.10
18	Road	45,104	1,785,662	15.52
19	Pond	85	36,205	0.31
20	River	307	99,704	0.87
	Total	104,342	11,507,390	100.00

2.4 METROS data

METROS is a system of weather observation equipment installed jointly by Tokyo Metropolitan University and the Tokyo Institute of Environmental Sciences in 126 locations inside of Tokyo. Fig. 3 shows the positions of METROS Observatories around the Upstream Kanda Watershed. There are a total of 16 observation points in the vicinity, two of them belong to the METROS20 system and fourteen of them belong to METROS100 observation stations. We perform a Thiessen split as shown in Fig. 3, then all the surface features are assigned the temperatures observed at the observatory in the Thiessen segments. Table 2 shows the monthly and daily average temperatures at each observation point. The average annual temperatures differ by as much as 1 ℃, from 16.37 ℃ at St. 1 to 17.36 ℃ at St. 8.

Table 2. Monthly and annual average temperatures at observation stations

Month	Observation point								
	St.1	St.2	St.3	St.4	St.5	St.6	St.7	St.8	St.9
	Monthly average temperature of the daily mean (℃)								
1	5.17	5.39	4.99	5.55	5.59	5.61	5.13	5.90	5.66
2	7.43	7.61	7.28	7.77	7.81	7.82	7.36	8.27	7.92
3	8.88	9.13	9.29	9.59	9.50	9.11	9.33	9.79	9.29
4	15.51	15.80	16.04	16.32	16.09	15.94	16.12	16.60	16.05
5	18.87	19.17	19.53	19.73	19.51	19.34	19.68	19.94	19.52
6	23.11	23.33	23.68	23.83	23.50	23.45	23.68	24.01	23.52
7	27.73	28.15	28.57	28.83	28.35	28.35	28.55	29.01	28.46
8	26.19	26.62	26.97	27.21	26.85	26.89	26.94	27.43	26.90
9	24.21	24.61	24.81	25.13	24.89	24.96	24.93	25.38	24.94
10	16.44	16.75	16.78	17.05	16.75	16.88	16.73	17.34	16.87
11	14.40	14.69	14.34	14.85	15.14	14.61	14.23	15.21	14.80
12	8.47	8.80	8.47	8.76	8.98	8.60	8.21	9.32	8.87
Annual average	16.37	16.68	16.74	17.06	16.92	16.80	16.75	17.36	16.91

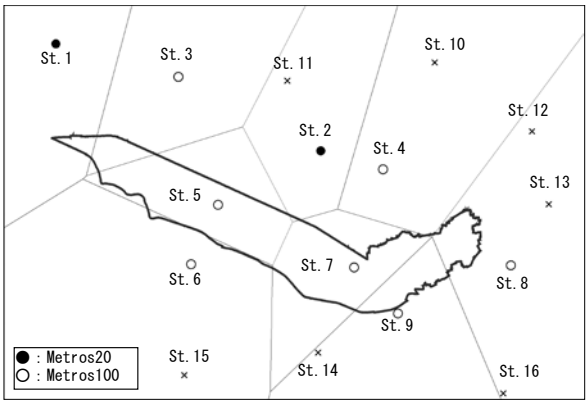

Figure 3. Locations of METROS installations around the target watershed

3 RESULTS AND DISCUSSION

3.1 Calculation conditions

We calculated the sensible heat and latent heat for each day unit for one year (January to December 2004), then we analyzed the temperatures in

individual land-surface features and evapotranspiration using the sensible and latent heats. For the average daily temperature used in the bulk formula, we used the observed values at each feature's position shown in Fig. 3.

In advanced GIS delineation there are 20 land use types as shown in Table 3. Each area is configured as impermeable (including water areas) or permeable. It should be noted that the area *Between roads* (except where there are buildings in the medians) was set as 50% permeable based on the results of a sample survey. For each land use type, the evapotranspiration coefficient k and saturated soil moisture content S_{sat} should be applicable for an evapotranspiration model that takes soil moisture into account.

Table 3 lists evapotranspiration parameters for the 20 land use types, which are divided into six groups within which the parameters are the same. The groups are 1: *Forest*; 2: *Field*; 3: *Parking* (permeable), *Athletic field* (permeable), *Grass*, *Park*, *Cemetery*, *Tennis court* (permeable) and *Between roads* (50% permeable); 4: *Bare land*; 5: *Building*, *Parking* (impermeable), *Athletic field* (impermeable), *Paved area*, *Rail*, *Between roads* (50% impermeable), *Tennis court* (impermeable) and *Road*. In group 5, direct outflow accrual was set to 2 mm, adopting a typical value. Water is assigned to group 6, which includes *Pool*, *Pond*, and *River*.

Table 3. Area, percentage area, and evapotranspiration parameters by land use

No.	Land use type	Infiltration Characteristic	Area	Percentage area	Saturated soil moisture content	Minimum soil moisture	Initial soil moisture	Evapo-transpiration coefficient	Albedo	Group
			(km^2)	(%)	*Ssat* (mm)	*Sn* (mm)	*S*(0) (mm)	*k*	α	
1	Building	Impermeable	3.38	29.39	-	-	-	-	0.12	Group 5
2	Parking (Permeable)	Permeable	0.06	0.52	92	74	64	0.34	0.10	Group 3
3	Parking (Impermeable)	Impermeable	0.21	1.80	-	-	-	-	0.12	Group 5
4	Athletic field (Permeable)	Permeable	0.23	1.96	92	74	64	0.34	0.10	Group 3
5	Athletic field (Impermeable)	Impermeable	0.02	0.20	-	-	-	-	0.12	Group 5
6	Forest	Permeable	1.04	9.05	138	110	97	4.38	0.15	Group 1
7	Grass	Permeable	0.17	1.49	92	74	64	0.34	0.10	Group 3
8	Field	Permeable	0.19	1.64	104	83	73	0.55	0.23	Group 2
9	Park	Permeable	0.10	0.91	92	74	64	0.34	0.10	Group 3
10	Cemetery	Permeable	0.07	0.61	92	74	64	0.34	0.10	Group 3
11	Paved area	Impermeable	0.38	3.30	-	-	-	-	0.12	Group 5
12	Rail	Impermeable	0.15	1.30	-	-	-	-	0.12	Group 5
13	Between roads	50% Permeable	3.43	29.83	92	74	64	0.34	0.10	Group 3
14	Tennis court (Permeable)	Permeable	0.05	0.47	92	74	64	0.34	0.10	Group 3
15	Tennis court (Impermeable)	Impermeable	0.03	0.26	-	-	-	-	0.12	Group 5
16	Bare land	Permeable	0.05	0.46	80	64	56	0.25	0.10	Group 4
17	Pool	Impermeable	0.01	0.10	-	-	-	-	0.12	Group 6
18	Road	Impermeable	1.79	15.52	-	-	-	-	0.12	Group 5
19	Pond	Impermeable	0.04	0.31	-	-	-	-	0.12	Group 6
20	River	Impermeable	0.10	0.87	-	-	-	-	0.12	Group 6

3.2 Results and discussion

Fig. 4 presents a time series of actual evapotranspiration, considering soil

moisture and potential evapotranspiration from each land use group in the region. The area assigned to St. 5 is used as a representative example, since that area contains the largest area of the watershed among the Thiessen divisions. Each group assigned the temperature observed at St. 5. Daily precipitation at St. 2 and the time series of average daily temperature at St. 5 are also shown together in Fig. 4. The average daily temperature peaks at St. 5 in July-August at about 30 °C, and potential evapotranspiration, calculated from the heat balance equation, is about 7 mm/day at maximum regardless of land use type. Actual evapotranspiration in late July is much smaller than potential evapotranspiration in *Forest* (group 1) and *Fields* (group 2) as shown in Fig.4a) and b). This is because evaporation efficiency β is small since soil moisture drops due to evapotranspiration and little rainfall in July. On the other hand, for *Buildings*, an impermeable area, (group 5 in Fig. 4e), the maximum evapotranspiration is 2 mm/day because direct rainfall more than 2 mm (which is set as the limit for depression storage) becomes outflow.

Table 4 shows the total annual evapotranspiration for each group, calculated from the average annual temperature of 9 observation points and average daily temperatures in individual observation points. Where no value is presented, the corresponding land use type does not appear in that station's area. Table 4 shows that changes in evapotranspiration due to differences in land use do not vary with the temperature of the observation point. The average value of annual evapotranspiration is highest for *Rivers*, followed by *Forest*, *Fields*, *Grass*, *Bare land* and *Buildings*. Table 4 shows that higher annual evapotranspiration results from higher temperatures regardless of the land use type. For example, the annual evapotranspiration for forest (group 1), is 716.0 mm/year at St. 8, which has the highest annual average temperature of the 9 observation points (17.36 °C), but only 679.7 mm/year at St. 1, which has the lowest annual average temperature (16.37 °C). A difference of about 36 mm/year results from a difference of about 1 °C of annual average temperature.

The difference between the observed temperatures and the land surface temperature on July 21 for each element are shown in Fig. 5, which had the highest temperature for any observed point during the year. Fig. 5 shows that there are large areas with features having surface temperatures lower than the air temperature (negative values) in the area where observations from St. 8 are used to calculate evapotranspiration. This is because St. 8 has the highest average temperatures of all 9 observation points (See Table 4). Table 4 suggests that calculated evapotranspiration and latent heat transport increase when the observed temperature increases. The table also suggests that, for forest, evapotranspiration increases significantly, and the ground surface temperature drops.

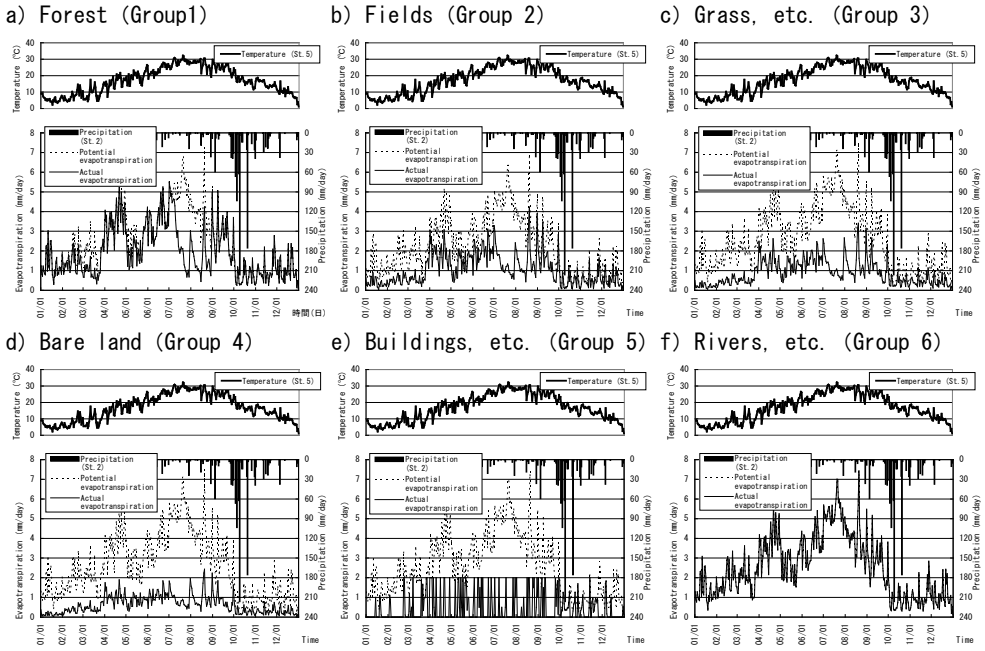

Figure 4. Evapotranspiration for each land use group (using temperature at St.5)

Table 4. Annual evapotranspiration for each land use type and annual mean temperature at observatory

Item	Observation Point	Annual average Temperature ℃	Forest (Group 1)	Fields (Group 2)	Grass, etc. (Group 3)	Bare land (Group 4)	Buildings, etc. (Group 5)	Rivers, etc. (Group 6)
Annual Evapotranspiration (mm/year)	St.1	16.37	679.7	373.6	308.8	-	159.9	-
	St.2	16.68	-	-	-	-	161.3	-
	St.3	16.74	694.5	383.9	317.6	231.3	162.5	921.3
	St.4	17.06	-	-	-	-	162.7	-
	St.5	16.92	701.0	386.7	319.2	232.6	161.7	928.3
	St.6	16.80	696.0	384.0	317.3	-	162.2	-
	St.7	16.75	694.6	383.9	317.8	231.5	161.8	922.3
	St.8	17.36	716.0	-	327.3	239.3	163.5	960.6
	St.9	16.91	699.5	386.0	318.8	232.4	161.9	928.0
	Average	16.84	697.3	383.0	318.1	233.4	161.9	932.1

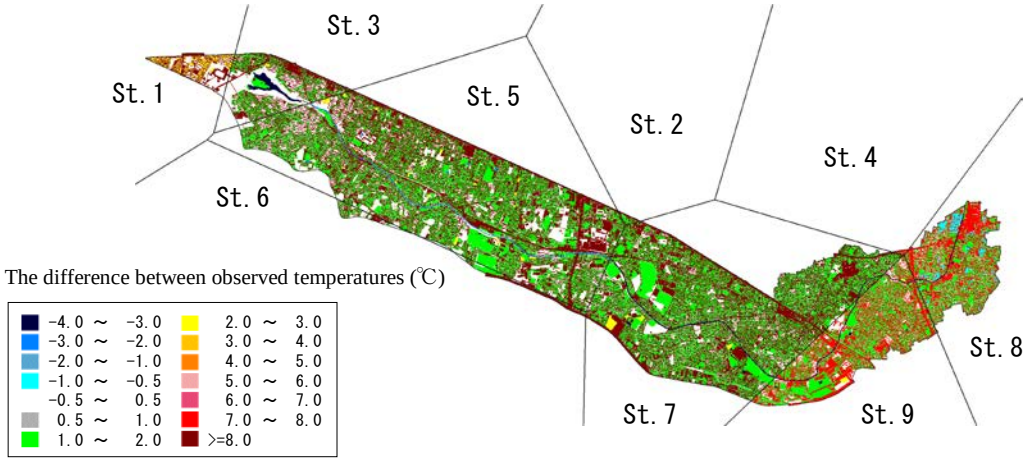

Figure 5. Surface temperature distribution map for July 21

4 CONCLUSIONS

In this paper, we estimated evapotranspiration, latent heat and sensible heat for individual land-surface features using the TET model, which takes the state of soil moisture into consideration. As a result, we confirmed that it was possible to estimate the latent heat, sensible heat, evapotranspiration of the earth surface features based on changing temperature in individual locations to correspond to land-surface features. In addition, it was possible to ascertain the spatial distribution of the differences in surface temperature and evapotranspiration for features in the Upstream Kanda Watershed.

ACKNOWLEDGEMENTS: I would like to acknowledge the contributions of Prof. Akira Kawamura in carrying out this study, "Research on adaptation measures for solving water problems in Asian urban areas" Tokyo Asia advanced research. In addition, we used METROS data provided by the Tokyo Metropolitan Institute of Environmental Sciences. We would like to express our sincere gratitude for their valuable contributions to the study.

REFERENCES

Amaguchi, H., Kawamura, A., Takasaki, T.: Physically based distributed flood runoff model for an urban catchment using polygon feature GIS data, *J. Jpn. Soc. Civ. Eng.*, **63 (3)** , 206-223 (2007) (in Japanese).

Amaguchi, H., Kawamura, A., Araki, K., Takasaki, T.: Development of storm runoff model using advanced GIS delineation for upper Kanda basin and its application, *Advances in River Engineering*, **15** , 377-382 (2009) (in Japanese).

Amaguchi, H., Kawamura, A., Takasaki, T. Nakagawa, N.: A proposal of Tokyo Storm Runoff Model for an urban catchment using urban landscape GIS delineation, *J. Jpn. Soc. Civ. Eng. Ser. B1*, **67 (4)** , 517-522 (2011) (in Japanese).

Hamon,W.R.: Estimating Potential Evapotranspiration, *J. Hydraulics Div. Proc. Am. Soc. Civil. Eng.*, **87**, 107-120 (1961) .

Koga, T., Kawamura, A., Amaguchi, H.: Modeling the evapotranspiration using advanced GIS delineation and its application to urban river basin, *J. Jpn. Soc. Civ. Eng. Ser. B1*, **69 (4)** , 1771-1776 (2013) (in Japanese).

Koga, T., Kawamura, A., Amaguchi, H.: Modeling the evapotranspiration of individual land-surface features considering heat balance and soil moisture, and its application to an actual river basin, *J. Jpn. Soc. Civ. Eng. Ser. B1*, **70 (4)** , 319-324 (2014) (in Japanese) .

Thornthwaite,C.W.: An approach toward a rational classification of climate, *Geographical Review*, **38**, 55-94 (1948).